Optimization of Single-Zone Drying of Polymer Solution Coatings Using Mathematical Modeling

PETER E. PRICE, JR.,[1] RICHARD A. CAIRNCROSS[2]

[1] 3M Engineering Systems Technology Center, Building 518-1-01, St. Paul, Minnesota 55144

[2] Drexel University, Chemical Engineering Department, Philadelphia, Pennsylvania 19104

Received 4 February 1999; accepted 10 November 1999

ABSTRACT: Optimal conditions for drying polymer–solvent coatings result from a trade-off between minimizing the residual solvent level and creating defects. This article describes an application of automated constrained optimization with a detailed mathematical drying model to find the optimal drying conditions for a prototypical coating in a single-zone oven. The optimization process seeks oven conditions that minimize the residual solvent level for a fixed oven residence time without boiling the solvent within the coating. The optimal oven conditions include the air temperature and coating-side and substrate-side heat-transfer coefficients. The conditions are constrained to physically reasonable values. According to our results, the optimal coating-side heat-transfer coefficient is always equal to or greater than the optimal substrate-side heat-transfer coefficient. © 2000 John Wiley & Sons, Inc. J Appl Polym Sci 78: 149–165, 2000

Key words: drying model; polymer-solution coatings; optimization; defects; diffusion

INTRODUCTION

Many industrial and consumer products are thin coatings prepared by spreading polymer–solvent solutions onto moving webs; for example, adhesive tapes, magnetic media, paints, protective coatings, and imaging coatings are often produced this way. After deposition, the solvent is typically removed from the coating in parallel flow, impingement, or floatation driers. Drying is frequently the last process that can affect the properties of a coated web. Improper drying conditions can create a variety of drying-induced defects such as blisters, warping, mottle, cracks, and crazing. Improper drying conditions can also lead to insufficient solvent removal from the coating. Thus, the choice of drying conditions often means the difference between generating a high-quality, salable product and generating an unusable product. In addition, drying requires massive amounts of energy to heat the drying gas and so has high operating costs. Drying equipment also represents one of the greatest capital expenditures for the production of coated webs. In the design of drying systems and the choice of drying conditions, there is often a trade-off between the desire to produce a defect-free product at high speeds (which leads to long driers and high energy costs) and process economics. For a given drier length, it is important to optimize the drier design and drying conditions.

In the coating industry, the operating conditions for driers are usually determined by a combination of experimentation, heuristics from prior experience, and statistical analysis. The question frequently arises as to whether the drying conditions are optimal. The answer to this question requires a clear definition of what results are

Correspondence to: R. A. Cairncross.

Journal of Applied Polymer Science, Vol. 78, 149–165 (2000)

optimal; for example, optimal conditions could maximize profits or minimize costs. In this article, we consider a drier to be operating at optimal conditions when it minimizes the residual solvent in the film for a specified web speed. However, the search for an optimum is subject to constraints on heat-transfer rates and avoidance of defects. For practical purposes, varying air flow in a drier can only change the effective heat-transfer coefficient from $\sim 10^{-4}$ cal cm^{-2} s^{-1} °C^{-1} for stagnant air to $\sim 4 \times 10^{-3}$ cal cm^{-2} s^{-1} °C^{-1} for high-velocity impingement driers.[1] In this article, we define defects as blisters or bubbles that occur by boiling of the solvent. This constrained optimization problem is closely related to the problem of finding the maximum line speed to reach a specified residual level.

There are many other processes that can occur simultaneously with drying (e.g., curing, particle migration, elastic stresses) and can also affect the product quality. A drying model that includes these processes would be significantly more complex than the model presented here. In practice, these additional processes could require drying conditions that are less than optimal, as presently defined.

This article describes a method for optimizing drier heat-transfer coefficients, which relate to air-flow rates, and drier air temperature in order to minimize solvent retention without boiling the solvent within the coating. We used a detailed mathematical model of solvent diffusion and heat conduction within the coating and found numerical solutions to the model equations using the finite element method. We applied the model to drying of a prototypical coating consisting of a poly(vinyl acetate)/toluene solution on a polyester web. The results for a base case using typical drying conditions demonstrate why optimal drying conditions do not always correspond to high oven temperatures and high air flows. This is not a complete analysis for all coatings, but the qualitative results for this particular system should extend to many other systems.

The next section describes a method for using the drying model to automatically find optimal drying conditions. This method predicts the oven temperature, coating-side heat-transfer coefficient, and substrate-side heat-transfer coefficient which produces the lowest residual solvent level without blisters. The results appear to contradict the widely held notion that higher substrate-side heat-transfer coefficients, that is, "backside drying," are preferable for blister prone coatings. However, *nearly optimum* conditions can exist with high substrate-side heat-transfer coefficients and low coating-side heat-transfer coefficients. In some cases, such conditions are certainly preferable to the high heat-transfer coefficients on both sides of the web that typically occur in floatation ovens.

The optimal drying conditions are sensitive to other operating and physical parameters such as coating weight, percent solids, solvent diffusivity, and oven residence time. Optimization calculations over a range of these parameters show that the optimum coating-side heat-transfer coefficients are always equal to or greater than the optimum substrate-side heat-transfer coefficients. However, there are conditions where, unlike the results described above, high heat-transfer coefficients on both sides of the web are preferable to a "backside drying" approach.

MODEL

Drying Model

Drying involves simultaneous mass, energy, and momentum transport. In many practical cases, the equations reduce to one-dimensional mass and energy transport. Detailed drying models have received considerable attention, most notably by Robinson et al.,[2] Roehner,[3] Yapel,[4] Cairncross et al.,[5] Vrentas and Vrentas,[6] and Aust et al.[7] These drying models predict heat and mass transport within a thin slice of a binary polymer–solvent coating on an impermeable substrate (web), shown schematically in Figure 1. The coating thickness and temperature and solvent concentration profiles evolve as the coating/web system moves through the drying oven.

Conservation of Mass

Neglecting chemical reactions and assuming that there is no volume change on mixing (ideal solution), the solvent mass balance in the coating phase is

$$\frac{\partial c_S}{\partial t} = \frac{\partial}{\partial x}\left(D\,\frac{\partial c_S}{\partial x}\right) \tag{1}$$

$c_S(x, t)$ is the solvent concentration in the polymer phase in units of mass per volume; t, the time; x, the vertical position in the coating; $D(c_S$,

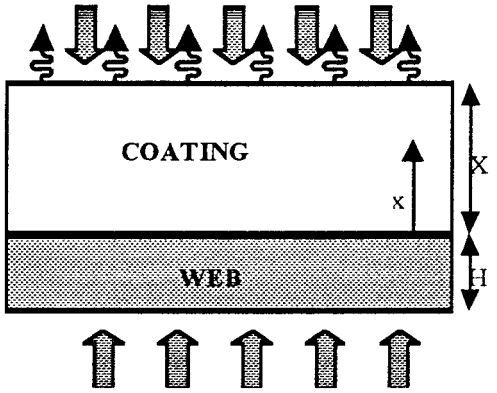

Figure 1 Diagram of a typical coating/substrate system. The coating thickness is X and the substrate thickness is H. Blowing air supplies heat to the top of the coating and the bottom of the substrate. The blowing air also removes solvent from the top of the coating.

T), the solvent–polymer mutual diffusion coefficient; and T, the temperature.

The value of the diffusion coefficient characterizes how quickly a solvent can transport to the surface. Several authors have shown that correct prediction of how the diffusion coefficient varies with the temperature and solvent concentration is critical to accurate predictions of the drying process. In particular, as the polymer concentration increases, diffusion is hindered by low mobility of the polymer molecules, and the mutual diffusion coefficient can decrease by several orders of magnitude. We use the Vrentas and Duda[8,9] free-volume theory to describe the concentration and temperature dependence of the mutual diffusion coefficients:

$$D = QD_0 \exp\left(-\frac{E}{RT}\right)\exp\left(-\frac{\gamma(w_S\hat{V}_S^* + w_P\xi\hat{V}_P^*)}{\hat{V}_{\mathrm{FH}}}\right) \tag{2}$$

D_0 is a preexponential factor; E, the activation energy; R, the gas constant; $\hat{V}_S^*$ and $\hat{V}_P^*$, the solvent and polymer specific critical hole free volumes; ξ, the ratio of the solvent and polymer critical molar jumping unit volumes; w_S and w_P, the mass fractions of solvent and polymer; and Q, a thermodynamic parameter that converts the self-diffusion coefficient into the mutual diffusion coefficient:

$$Q = (1 - \phi_S)^2(1 - 2\chi\phi_S) \tag{3}$$

ϕ_S is the volume fraction of solvent; χ, the Flory–Huggins parameter; and $\hat{V}_{\mathrm{FH}}$, is the free volume available for diffusion:

$$\frac{\hat{V}_{\mathrm{FH}}}{\gamma} = \frac{K_{11}}{\gamma} w_S(K_{21} + T - T_{gS}) + \frac{K_{12}}{\gamma} w_P(K_{22} + T - T_{gP}) \tag{4}$$

K_{11}/γ and $K_{21} - T_{gS}$ are free volume parameters for the solvent, and K_{12}/γ and $K_{22} - T_{gP}$, free volume parameters for the polymer. Mass fractions, $w_i = c_i/(c_S + c_P)$, and volume fractions, $\phi_i = c_i\hat{V}_i$, are related to c_i by ideal solution behavior with $\hat{V}_i$, the specific volume of pure species i.

The initial solvent concentration is assumed uniform:

$$c_S(x, 0) = c_S^0 \tag{5}$$

The coating has an initial thickness $X(0) = L$.

The substrate (web) is impermeable, so the concentration gradient must be zero at the coating/substrate interface:

$$\frac{\partial c_S}{\partial x} = 0 \qquad x = 0 \tag{6}$$

The solvent flux through the top coating surface (i.e., the evaporation rate) is the result of an interfacial mass balance. We use a mass-transfer coefficient, k_G, to characterize the mass transport in the external gas:

$$-D\frac{\partial c_S}{\partial x} + c_S\frac{dX}{dt} = -k_G(P_S^G - P_S^{G\infty}) \qquad x = X(t) \tag{7}$$

P_S^G is the equilibrium solvent pressure at the coating/air interface, and $P_S^{G\infty}$, the solvent pressure in the bulk air. The left-hand side of eq. (7) represents the rate of solvent flux relative to the moving surface, which must equal the flux in the gas phase. The mass-transfer coefficient is calculated by analogy with a heat-transfer coefficient, as discussed below.

The solvent partial pressure at the surface is the product of the vapor pressure of pure solvent at the current temperature multiplied by the activity of the solvent at the current polymer phase solvent concentration. We assume that the Flory–Huggins equation describes the solvent activity:

$$P_S^G = P_S^* \phi_S \exp(\phi_P + \chi \phi_P^2) \tag{8}$$

χ is the Flory–Huggins interaction parameter. The Antoine equation describes the pure component vapor pressure:

$$\log(P_S^*) = A - \frac{B}{T + C} \tag{9}$$

A, B, and C are Antoine coefficients.

The evaporation rate also sets the rate of film shrinkage by a volume balance at the coating surface:

$$\frac{dX}{dt} = -k_G \hat{V}_S (P_S^G - P_S^{G\infty}) \qquad x = X(t) \tag{10}$$

$\hat{V}_i$ is the specific volume of the pure solvent. Equations (1)–(10) form a complete description of the evolution of solvent concentration and coating thickness through a drier.

Conservation of Energy

Industrial drying of coatings typically involves blowing hot air on the coating/substrate system to accelerate the rate of drying. Energy flows through the coating and substrate by conduction:

$$\frac{\partial \rho \hat{H}(T)}{\partial t} = \frac{\partial}{\partial x}\left(\kappa \frac{\partial T}{\partial x}\right) \tag{11}$$

$\hat{H}(T)$ is the enthalpy of the material per unit mass; κ, the thermal conductivity; and ρ, the density. In this equation, the convective transport of energy with the mass-averaged motion of the material is neglected. This assumption is justified, because even if the mass average velocity is not zero, thermal diffusion is much faster than mass diffusion in most coating applications (i.e., Le $\gg 1$), so *convective* heat transfer in the coating is small.

The enthalpy is normally expanded as the product of the specific heat multiplied by the temperature difference between the material and a reference value. In the substrate or web, the density, specific heat, and thermal conductivity are essentially constant, so the energy balance simplifies to

$$\rho_W \hat{C}p_W \frac{\partial T}{\partial t} = \kappa_w \frac{\partial^2 T}{\partial x^2} \tag{12}$$

ρ_w, $\hat{C}p_W$, and κ_W are the density, specific heat, and thermal conductivity of the substrate, respectively. The energy balance for the coating is

$$\rho_c \hat{C}p_c \frac{\partial T}{\partial t} = \frac{\partial}{\partial x}\left(\kappa_c \frac{\partial T}{\partial x}\right) \tag{13}$$

ρ_C, $\hat{C}p_c$, and κ_C are the density, specific heat, and thermal conductivity of the coating, respectively. In this equation, the enthalpy of the polymer–solvent solution is assumed to be a sum of the enthalpy of the polymer and solvent components (i.e., no heat of mixing).

The initial temperature in the polymer and substrate phases is uniform at $T(x, 0) = T^0$. We assume that energy flux to the lower substrate surface is described by the substrate-side heat-transfer coefficient, h_W:

$$-\kappa_w \frac{\partial T}{\partial x} = -h_w (T - T^\infty) \qquad x = -H \tag{14}$$

At the coating/web interface, the energy flux and temperature are both continuous:

$$-\kappa_W \frac{\partial T_W}{\partial x} = -\kappa_C \frac{\partial T_C}{\partial x} \qquad x = 0 \tag{15}$$

$$T_W = T_C \qquad x = 0 \tag{16}$$

The energy flux to the upper surface of the coating is the result of an interfacial energy balance including the effect of evaporative cooling. We use the coating-side heat-transfer coefficient, h_C, to characterize the energy transport from the surrounding air:

$$-\kappa_C \frac{\partial T}{\partial x} = -h_C (T - T^\infty) + \Delta H_{VS} k_G (P_S^G - P_S^{G\infty}) \qquad x = X \tag{17}$$

Here, ΔH_{VS} is the heat of vaporization of the solvent.

The heat and mass-transfer coefficients are related by the Chilton–Coburn analogy:

$$\frac{h_C M_S}{k_G} = \rho_{air} \hat{C}p_{air} R\bar{T}\left(\frac{\rho_{air} \hat{C}p_{air} D_{air}}{\kappa_{air}}\right)^{-0.67} \tag{18}$$

M_S is the solvent molecular weight; ρ_{air}, $\hat{C}p_{air}$, and κ_{air} are the density, specific heat, and ther-

mal conductivity of the air evaluated at the average temperature, $\bar{T} = (T + T^{\infty})/2$, and D_{air}, the diffusivity of the solvent in air at the average temperature.

Numerical Methods

The numerical methods for solving this system of equations were discussed in detail elsewhere.[5,10] To obtain approximate solutions to the set of coupled nonlinear ordinary and partial differential equations that comprise the drying model, eqs. (1), (12), and (13) are discretized in space with the Galerkin finite element formulation using piecewise linear basis functions.[11] This discretization produces a set of ordinary differential equations that are integrated using DASSL,[12] an efficient solver for systems of stiff nonlinear ordinary differential-algebraic equations. The discretization and time-step error tolerances were tested for convergence under refinement. We used 30 unequally spaced elements and set the error tolerance in DASSL to 10^{-5}.

Typical Drying Profiles

Optimal drying conditions result from complex interactions among solvent transport, energy transport, materials properties, and process conditions. This section demonstrates typical drying behavior of polymer–solvent coatings; of particular interest are the *residual solvent* content in the coating (i.e., the solvent concentration integrated through the film thickness) and *average web temperature* (average temperature of coating and substrate). The polymer–solvent system used in these predictions is poly(vinyl acetate) in toluene, which is a model system typical of adhesive coatings. The physical properties of poly(vinyl acetate) and toluene are well known and are listed in Table I. The free-volume theory diffusion parameters were obtained by regression analysis of bench-top experiments.[13] Our base-case coating has a dry weight of 4.19×10^{-3} g/cm^2 of poly(vinyl acetate) and rests on a 3.56×10^{-3} cm (1.4 mil) polyester backing. The initial coating contains 30% solids by weight in toluene.

Figure 2 shows typical evolution of the residual solvent and average web temperature as a coated web passes through a single drying zone. The residual solvent, R_S, is the total solvent contained in the coating per unit area, which is equal to the integral of the solvent concentration through the coating thickness:

Table I Drying Model Parameters for Poly(vinyl acetate) and Toluene

Toluene Properties	
ρ_S (g/cm^3)	0.866
Cp_S (cal g^{-1} °C^{-1})	0.44
κ_S (cal/s^{-1} cm^{-1} °C^{-1})	$3.475 \cdot 10^{-4}$
M_S (g/mol)	92.14
$\Delta H_{\text{vap},S}$ (cal/g)	98.89
A	4.07383
B	1344.8
C	−53.668
χ	0.39
Poly(vinyl acetate) Properties	
ρ_P (g/cm^3)	1.17
Cp_P (cal g^{-1} °C^{-1})	0.35
κ_P (cal/s^{-1} cm^{-1} °C^{-1})	3.5×10^{-4}
Substrate Properties	
ρ_W (g/cm^3)	1.38
Cp_W (cal g^{-1} °C^{-1})	0.45
κ_W (cal s^{-1} cm^{-1} °C^{-1})	3.22×10^{-4}
H (cm)	3.556×10^{-3}
Diffusion Parameters	
D_0 (cm^2/s)	3.998×10^{-4}
E_a (cal/mol)	0.0
ξ	0.958
K_{11}/γ (cm^3 g^{-1} K^{-1})	2.21×10^{-3}
$K_{21} - T_{gS}$ (K)	−103.0
K_{12}/γ (cm^3 g^{-1} K^{-1})	6.145×10^{-4}
$K_{22} - T_{gP}$ (K)	−223.9
$\hat{V}_S^*$ (cm^3)	0.917
$\hat{V}_P^*$ (cm^3)	1.0

$$R_S = \int_0^{X(t)} c_S \, dx \tag{19}$$

Because the web moves at constant speed, the distance through the drier is converted to time since entering the drier. The curves show three distinct regions of drying behavior, which are commonly called warm-up, constant rate drying, and falling rate drying.

The *warm-up* region is the initial transient during which the coating enters the drier and the temperature increases rapidly until the rate of energy supplied by the air nearly matches the rate of energy consumption by evaporation (due to

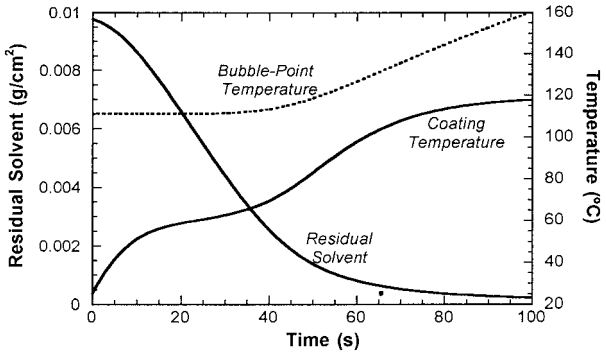

Figure 2 Example of drying of a poly(vinyl acetate)/toluene coating under low air flow. The oven temperature is 120°C, and the heat-transfer coefficients are both 2×10^{-4} cal cm^{-2} s^{-1} $°C^{-1}$. The coating initially contains 30% solvent by weight and the dry coating weight is 4.19×10^{-3} g/cm^2.

evaporative cooling). The duration of this warm-up region depends largely on the specific heat of the coating/substrate system, on the air flow rates (i.e., heat-transfer coefficients), and on the oven temperature.

When rate of energy supplied to the coating and the rate of evaporative cooling are nearly equal, the coating temperature and the rate of evaporation are nearly constant. This is called the *constant rate period* of drying (or more precisely, nearly constant rate period). The term *constant rate period* relates to drying of porous media in which the surface remains wet with the solvent during the early stages of drying. In porous media, the activity of the solvent is relatively insensitive to the initial decrease in solvent content, as long as the surface stays wet, and thus the drying rate remains practically constant. During drying of polymer–solvent coatings, the activity is more sensitive to solvent concentration, so the constant rate period more accurately corresponds to a case where the drying rate is slowly decreasing.

The *falling rate period* starts either when the solvent activity drops sharply (because the coating is running out of solvent) or when the rate of solvent diffusion to the surface drops. In polymer–solvent systems, the mutual diffusion coefficient is a strong function of concentration, so *diffusion-controlled drying* is normally the cause of the falling rate period. When drying becomes diffusion-controlled, the solvent concentration at the coating surface approaches equilibrium with the bulk gas-phase solvent concentration, typically near zero; the evaporation rate drops, and the web temperature increases to the oven temperature. This rapid increase in temperature at the onset of the falling rate period is a critical factor in the formation of blisters due to solvent boiling.

The duration and intensity of the three drying regimes depend upon the physical properties of the coating and the drying conditions. In some cases, the constant rate period is undetectable or appears as a small shoulder in the temperature increase. In other cases, the warm-up period is actually a cool-down period as evaporative cooling causes a drop in the web temperature. The results in Figure 2 correspond to coating-side and substrate-side heat-transfer coefficients of 2.0×10^{-4} cal s^{-1} cm^{-2} °C and an oven with 100 s of residence time. These values are typical of a low-velocity parallel flow drier. Under these conditions, the three distinct drying periods are all well defined.

Figure 2 also displays the *minimum bubble-point temperature* in the coating versus time. This bubble point results from computing the local bubble-point temperature at each point within the coating and finding the minimum value. The bubble-point temperature is the temperature at which the local equilibrium solvent partial pressure (as computed at a hypothetical internal interface) equals ambient pressure. A criterion for *blister* formation, which is adopted in this article, is that blisters form when the temperature anywhere within the coating exceeds the local bubble-point temperature. Figure 2 shows that the web temperature remains well below the bubble-point temperature, so blisters would not form under the base-case conditions.

Figure 3 shows solvent concentration profiles through the coating at a series of times corresponding to the same conditions as in Figure 2; the temperature profiles vary by less than 1 degree across the thickness of the coating and substrate and are not shown. Under the gentle drying conditions of this example, mild concentration gradients develop in the coating, with the highest solvent concentrations persisting at the coating/backing interface. The coating/backing interface is typically the location of the minimum bubble point within the coating, primarily because of the high solvent content there.

At higher heat-transfer rates, the energy consumption by evaporation never balances the energy supplied by the oven air. Under such conditions, the web temperature increases rapidly, without the leveling off that is indicative of the constant rate drying period. An example of this behavior is shown in Figure 4. The figure shows

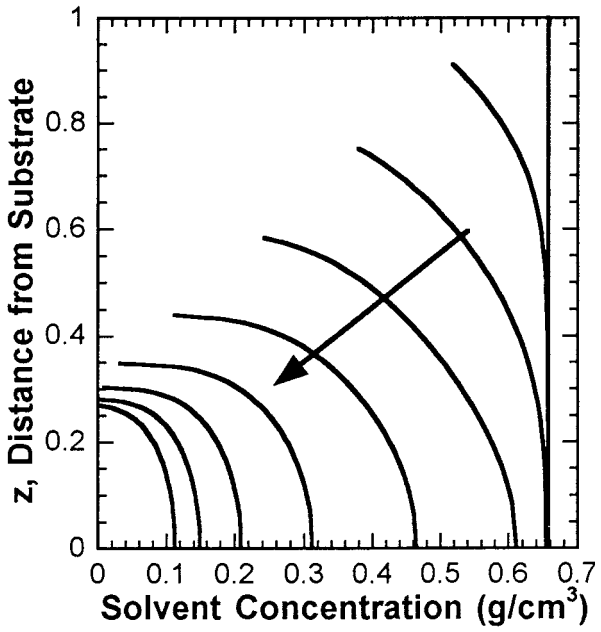

Figure 3 Concentration profiles of toluene corresponding to the conditions shown in Figure 2 for low air flow. Profiles are shown in 10-s increments starting at $t = 0$ when the solvent concentration is uniform.

the residual solvent and average web temperature profiles for the model system in an oven with coating-side and substrate-side heat-transfer coefficients of 2.0×10^{-3} cal s^{-1} cm^{-2} °C and all other parameters the same as used for Figure 2. These heat-transfer coefficients are typical of impingement or floatation ovens. Because of the fast temperature increase at these high heat-transfer rates, the coating approaches the bubble point of the solution more closely than it did for the low heat-transfer case.

Figure 5 shows solvent concentration profiles through the coating at a series of times for the same conditions as in Figure 4. At the high heat- and mass-transfer rates of this example, large concentration gradients develop immediately in the coating, a process sometimes referred to as *skinning*. At higher air flow rates, the web temperature increases to the oven temperature rapidly, while the solvent concentration remains high near the coating/substrate interface. Such conditions cause the coating temperature to approach the bubble-point temperature very rapidly.

Example of Optimal Drying

Optimal drying conditions, for the purposes of this article, are the accessible conditions that yield blister-free coatings and the lowest residual solvent for a particular oven residence time (or web speed). The formation of blisters is predicted whenever the coating temperature exceeds the bubble-point temperature. In real coating operations, dissolved or entrained air also contributes to blister formation, so blisters can form at coating temperatures below the bubble point. To optimize the drying process, a set of process conditions can be varied within ranges accessible to typical drying equipment. Heat-transfer coefficients typically range between 2×10^{-4} and 3.6×10^{-3} cal s^{-1} cm^{-2} $°C^{-1}$; these values correspond to oven configurations that vary from mild parallel flow to vigorous impingement. For the

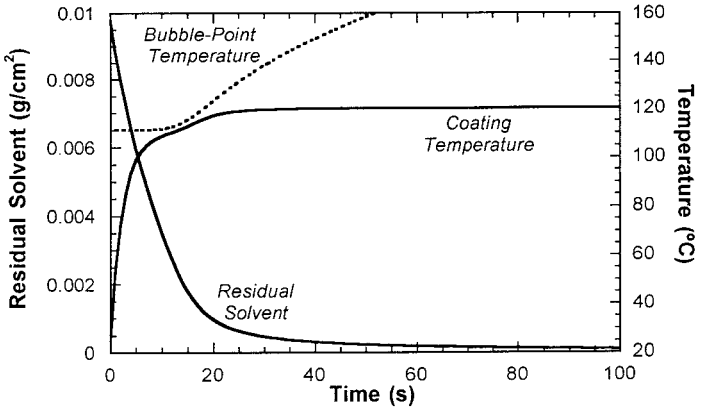

Figure 4 An example of drying of a poly(vinyl acetate)/toluene coating under high air flow. The oven temperature is 120°C, and the heat-transfer coefficients are both 2×10^{-3} cal cm^{-2} s^{-1} $°C^{-1}$. The coating initially contains 30% solvent by weight and the dry coating weight is 4.19×10^{-3} g/cm^2.

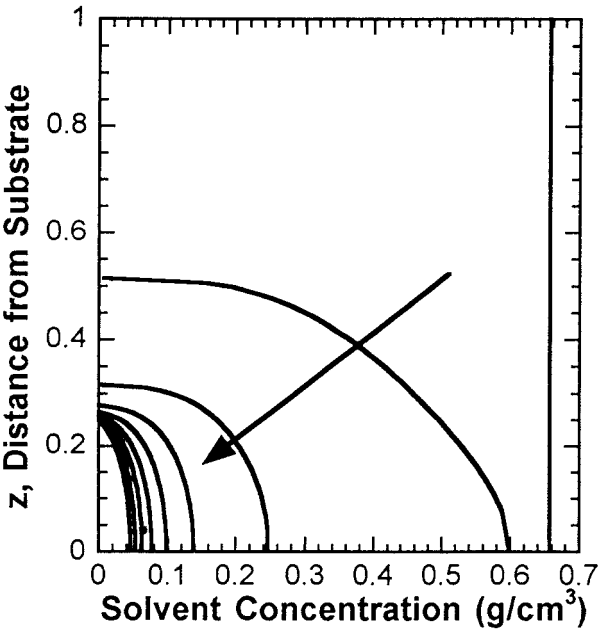

Figure 5 Concentration profiles of toluene corresponding to the conditions shown in Figure 4 for high air flow. Profiles are shown in 10-s increments starting at $t = 0$ when the solvent concentration is uniform.

remaining discussion, the oven residence time is set to 30 s.

To achieve the lowest residual solvent without blistering, the coating temperature must be nearly equal to the bubble-point temperature at some point within the oven; we call this the point of *near-blistering*. When near-blistering occurs, any increase in coating temperature, due to higher oven temperature or higher air flows, would cause blisters to form (see Figs. 6 and 7).

Figures 6 and 7 demonstrate why a hotter oven with lower substrate-side heat-transfer coefficients can yield a lower nonblistering residual solvent level. Figure 6 shows the average solvent content and web temperature profiles under high air flow ($h_W = 2.8 \times 10^{-3}$ cal s^{-1} cm^{-2} °C^{-1} and $h_C = 3.6 \times 10^{-3}$ cal s^{-1} cm^{-2} °C^{-1}) where the maximum allowable oven temperature is 118°C. The high heat-transfer rates in this case cause the temperature in the coating to approach the oven-zone temperature very quickly, much faster than solvent diffusion can reduce the solvent concentration near the base of the coating. The high external mass-transfer rates cause sharp concentration gradients in the coating (similar to Fig. 5). The elevated temperature and high solvent concentration at the bottom of the coating led to *near-blistering* very early in the oven, at approximately 10 s. In this case, the maximum allowable oven temperature (118°C) is only slightly higher than the bubble point of the initial solution (111°C).

At lower air flow, the approach to near-blistering is delayed. Figure 7 shows the average solvent content and web temperature profiles under low air flow ($h_W = 2.0 \times 10^{-4}$ cal s^{-1} cm^{-2} °C^{-1}, and $h_C = 2.6 \times 10^{-3}$ cal s^{-1} cm^{-2} °C^{-1}), where the maximum allowable oven temperature is 126°C. Again, these conditions produce a web temperature just below the bubble temperature. In this case, the oven temperature (126°C) is significantly higher than is the bubble point of the ini-

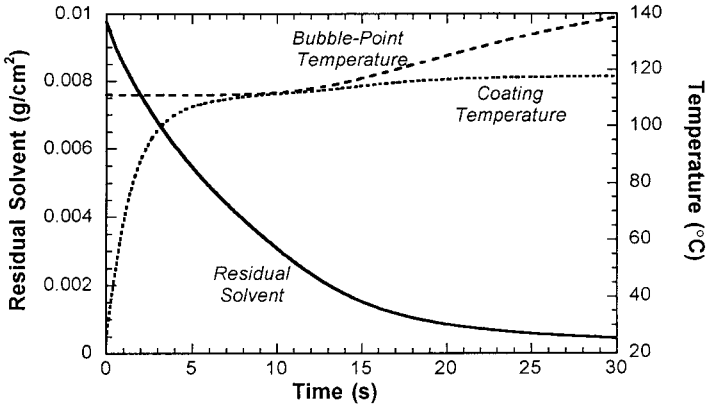

Figure 6 Drying under locally optimal conditions for an oven temperature of 118°C. The coating is initially 30 wt % poly(vinyl acetate) in toluene and the dry coating weight is 4.19×10^{-3} g/cm^2. The heat-transfer coefficients are $h_W = 2.8 \times 10^{-3}$ cal s^{-1} cm^{-2} °C^{-1} and $h_C = 3.6 \times 10^{-3}$ cal s^{-1} cm^{-2} °C^{-1}.

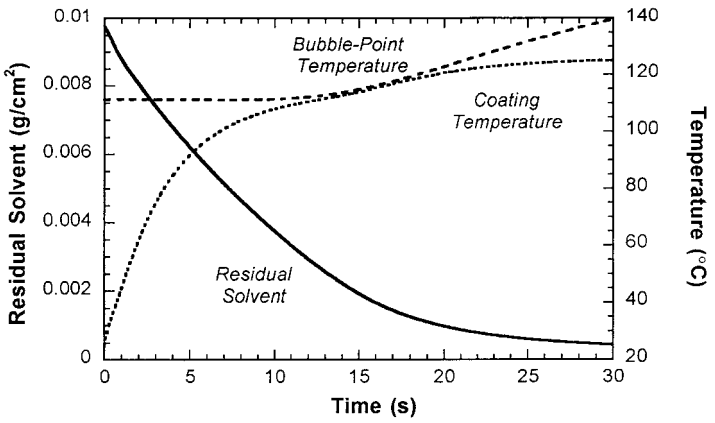

Figure 7 Drying under locally optimal conditions for an oven temperature 126°C. The coating is initially 30 wt % poly(vinyl acetate) in toluene and the dry coating weight is 4.19×10^{-3} g/cm^2. The heat-transfer coefficients are $h_W = 2 \times 10^{-4}$ cal s^{-1} cm^{-2} °C^{-1} and $h_C = 2.6 \times 10^{-3}$ cal s^{-1} cm^{-2} °C^{-1}.

tial solution (111°C). Although the oven temperature is higher, the lower heat-transfer coefficients cause slower heating and allow more time for the solvent to diffuse through the coating. Thus, near-blistering occurs later, at approximately 15 s.

In this low air-flow case, a higher oven temperature is allowed because the temperature increases more slowly. At low air flow, the point of near-blistering occurs after the bubble-point temperature starts to increase, and the coating ultimately reaches a higher temperature than in the high air-flow case. The higher temperature allows faster solvent diffusion and ultimately a lower residual solvent level.

Automatic Calculation of Optimal Conditions

The examples discussed in the last section show how the final residual solvent levels respond to changes in oven temperature and air flow (heat-transfer coefficients). They also suggest that the minimum allowable residual solvent level without blisters occurs under low air flow and high temperature. To find that minimum requires extensive trial and error calculation or automated optimization.

We use a modified Levenberg–Marquardt nonlinear least-squares regression to locate the optimum heat-transfer coefficients as a function of oven temperature. The global optimum is the oven temperature which gives the lowest optimal residual solvent.

The optimization routine minimizes the following objective functions:

$$\Omega_1 = w_{\text{boil}}(p_{s,\max} - p_{\text{boil}}) \qquad \text{if } p_{s,\max} > p_{\text{boil}} \tag{20}$$

$$\Omega_2 = w_{\text{res}} \int_0^{X(t_{\text{final}})} c_S \, dz + \begin{cases} w_{ht}(h_{\min} - h_{\text{bot}}) & h_W < h_{\min} \\ w_{ht}(h_{\min} - h_{\text{top}}) & h_C < h_{\min} \\ w_{ht}(h_{\text{bot}} - h_{\max}) & h_W > h_{\max} \\ w_{ht}(h_{\text{top}} - h_{\max}) & h_C > h_{\max} \end{cases} \tag{21}$$

The first function forces the web temperature to approach the bubble-point temperature somewhere within the drier. $w_{\text{boil}} = 10^6$ is a penalty weighting for this objective; $p_{s,\max}$, the maximum solvent partial pressure obtained in the drier; and p_{boil}, the partial pressure at which bubbles occur (1.0 atm). The second function minimizes the residual solvent level subject to the practical achievable limits of the coating-side and substrate-side heat-transfer coefficients ($h_{\min} = 2 \times 10^{-4}$ cal s^{-1} cm^{-2} °C^{-1} and $h_{\max} = 3.6 \times 10^{-3}$ cal s^{-1} cm^{-2} °C^{-1}). $w_{\text{res}} = 10^6$ and $w_{\text{ht}} = 10^8$ are penalty weightings.

The optimization code uses the computer code for the drying model as a subroutine for LMDIF1,[14] the modified Levenberg–Marquardt optimization routine. Given a coating configuration, materials parameters, and a temperature range, the code steps through a series of oven temperatures. At each oven temperature, the code locates the optimum coating-side and substrate-side heat-transfer coefficients by minimizing the objective functions in eqs. (20) and (21).

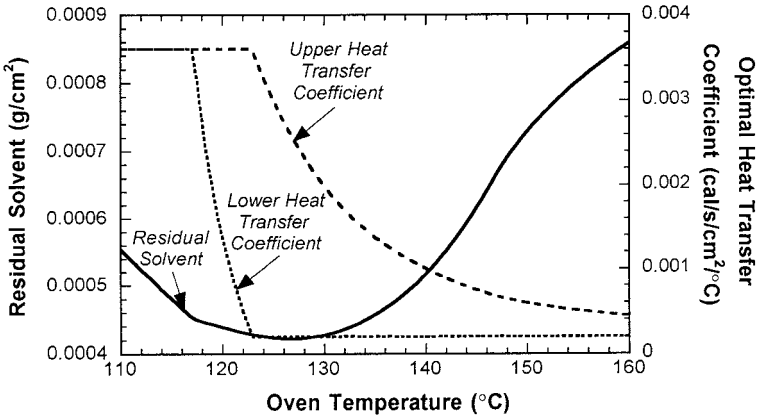

Figure 8 Locally optimal heat-transfer coefficients as a function of oven temperature. The coating is initially 30 wt % poly(vinyl acetate) in toluene and the dry coating weight is 4.19×10^{-3} g/cm^2. The oven residence time is 30 s. The global minimum in residual solvent occurs at about 126°C.

Figure 8 shows the local optimal heat-transfer coefficients as functions of oven temperature. At oven temperatures near or below the bubble-point temperature of the initial coating (below 118°C), the internal solvent partial pressure remains below the ambient pressure even at the highest heat-transfer rates, and bubbles cannot form. In this limit, the minimum residual solvent occurs when the heat-transfer coefficients are at the maximum allowable values. In this limit, the residual solvent at the local optimum decreases as oven temperature increases because higher temperature causes faster diffusion and higher solvent partial pressure. At oven temperatures well above the bubble-point temperature of the initial coating (above 140°C), low heat-transfer coefficients are required to avoid blistering. In this limit, the residual solvent at the local optimum increases as oven temperature increases because lower heat-transfer coefficients correspond to lower mass-transfer coefficients. Between the two limits is the global optimum which balances the goals of rapid drying and avoiding blisters.

At all oven temperatures, the optimal coating-side heat-transfer coefficient is always greater than or equal to the optimal substrate-side heat-transfer coefficient; this result is caused by the coupling between external heat transfer and mass transfer. On the top side of the coating, heat transfer and mass transfer are coupled by the Chilton–Coulburn analogy , but on the substrate side, there is no mass transfer so heat transfer and mass transfer are decoupled. Optimal avoidance of blistering is achieved by controlling the rate of heating while maintaining the mass-transfer rate as high as possible. This goal is achieved by first decreasing the substrate-side heat-transfer coefficient, and then, if necessary, decreasing the coating-side heat-transfer coefficient (and, consequently, the coating-side mass-transfer coefficient).

The global optimum (lowest residual solvent) occurs at an oven temperature of 126°C, with substrate-side and coating-side heat-transfer coefficients of 2.0×10^{-4} and 2.78×10^{-3} cal s^{-1} cm^{-2} °C^{-1}, respectively. The minimum solvent residual is 4.26×10^{-4} g/cm^2. The optimal heat-transfer coefficients both decrease with increasing oven temperature. As temperature increases above 126°C, the optimal substrate-side heat-transfer coefficient does not change, but the optimal coating-side heat-transfer coefficient continues to decrease. The locations of these optima are sensitive to parameters as discussed in the following sections.

RESULTS AND DISCUSSION

Sensitivity of Optimal Conditions to Parameters

In the following sections, we examine the sensitivity of the optimal drying conditions to various process parameters. The comparisons are all made under a fixed oven residence time. The oven residence time sets the time scale for which the comparative statements are meaningful.

Coating Weight

The coating weight (or thickness) is a parameter often changed in practice to produce different

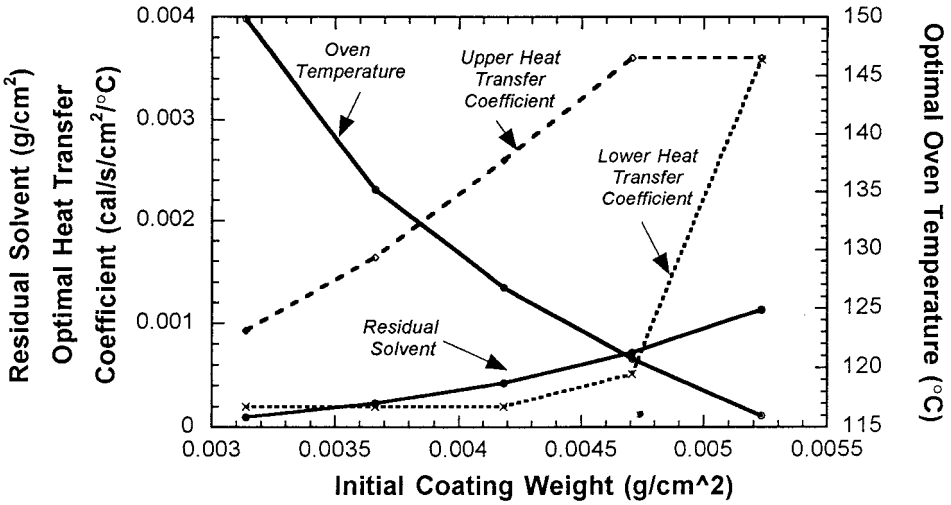

Figure 9 Globally optimal heat-transfer coefficients and oven temperature as a function of coating weight. The coating is initially 30 wt % poly(vinyl acetate) in toluene, and the oven residence time is 30 s.

products or to avoid defects. In addition, variation in coating weight occurs naturally through fluctuations in the process, especially at start up and shut down. It is instructive to consider how the optimal drying conditions vary with coating weight between 3.14×10^{-3} and 5.23×10^{-3} g/cm^2, where the coating weight is defined as the mass of dry coating (pure polymer) per unit area. The initial coatings contain 30% solids, and the oven has a residence time of 30 s.

A common rule of thumb is that diffusion-limited drying rates scale with the square of the coating thickness. For polymer–solvent systems with concentration- and temperature-dependent diffusion coefficients, the rule of thumb is not strictly valid. However, thinner coatings are less restricted by diffusion rates than are thicker coatings. In addition, thinner coatings have less total mass and less solvent mass, which leads to more rapid heating. Thus, in thinner coatings, the residual solvent decreases more rapidly and blistering is less likely.

Figure 9 shows the globally optimal process conditions and final residual as functions of coating weight. The results show that the optimal residual solvent content is smaller in thinner coatings, as expected. Thicker coatings dry more slowly and require lower oven temperatures and higher air flow to obtain optimal drying conditions. The thickest coating requires the maximum heat-transfer coefficients of 3.6×10^{-3} cal s^{-1} cm^{-2} °C^{-1} and a fairly low oven temperature, 115.9°C. As the coating weight decreases, the globally optimum substrate-side heat-transfer coefficient rapidly decreases to its minimum allowable value, 2.0×10^{-4} cal s^{-1} cm^{-2} °C^{-1}, the globally optimum coating-side heat-transfer coefficient decreases gradually, and the optimum oven temperature increases. Table II summarizes the globally optimum conditions.

This decrease in the globally optimum heat-transfer coefficients with decreasing coating weight is counterintuitive from a mass-transfer perspective. Intuition suggests that thinner coat-

Table II Globally Optimal Conditions Versus Coating Weight

Coat Weight (g/cm^2)	h_W (cal s^{-1} cm^{-2} °C^{-1})	h_C (cal s^{-1} cm^{-2} °C^{-1})	T_{oven} (°C)	Residual Solvent (wt %)
3.14×10^{-3}	2×10^{-4}	9.29×10^{-4}	149.8	9.72×10^{-5}
3.66×10^{-3}	2×10^{-4}	1.65×10^{-3}	135.0	2.29×10^{-4}
4.19×10^{-3}	2×10^{-4}	2.59×10^{-3}	126.7	4.22×10^{-4}
4.71×10^{-3}	5.12×10^{-4}	3.6×10^{-3}	120.7	7.11×10^{-4}
5.23×10^{-3}	3.6×10^{-3}	3.6×10^{-3}	115.9	1.12×10^{-3}

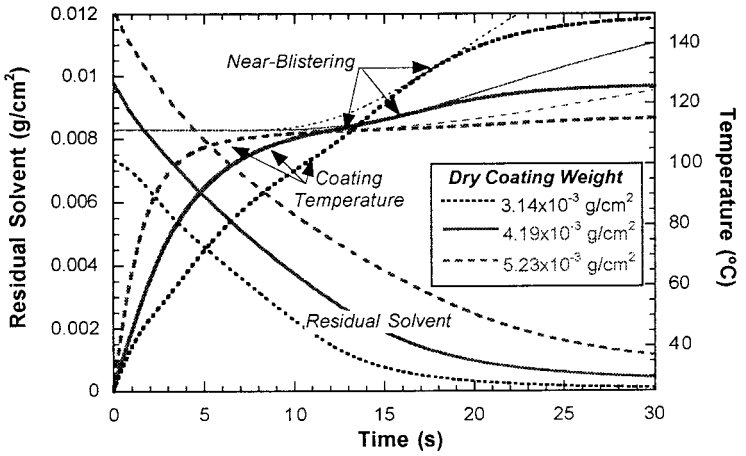

Figure 10 Drying profiles under globally optimal drying conditions for several coating weights corresponding to Figure 9. Bold lines indicate coating temperature and residual solvent, and thin lines indicate bubble-point temperature.

ings, which have less diffusional resistance, should have optimal drying conditions corresponding to the maximum practical heat/mass-transfer coefficients. This thinking, however, ignores thermal effects on the shape of the drying curve (as shown in Fig. 10). Thicker coatings have more total mass and more solvent mass; thus, they heat more slowly due to both heat capacity and evaporative cooling. In addition, thicker coatings retain higher solvent concentration near the bottom of the coating and are thus more susceptible to blistering for a longer time. These factors combine to shift the optimum conditions for thicker coatings to higher heat-transfer coefficients and lower temperatures compared to thinner coatings. Figure 10 shows that in thinner coatings the near-blistering point under optimal drying conditions occurs later, after the bubble-point temperature starts to increase.

Initial Solids Content

Changing the initial solids content of the coating solution directly affects the diffusional resistance to drying. In coatings with higher solids content, the diffusion coefficients are lower and the onset

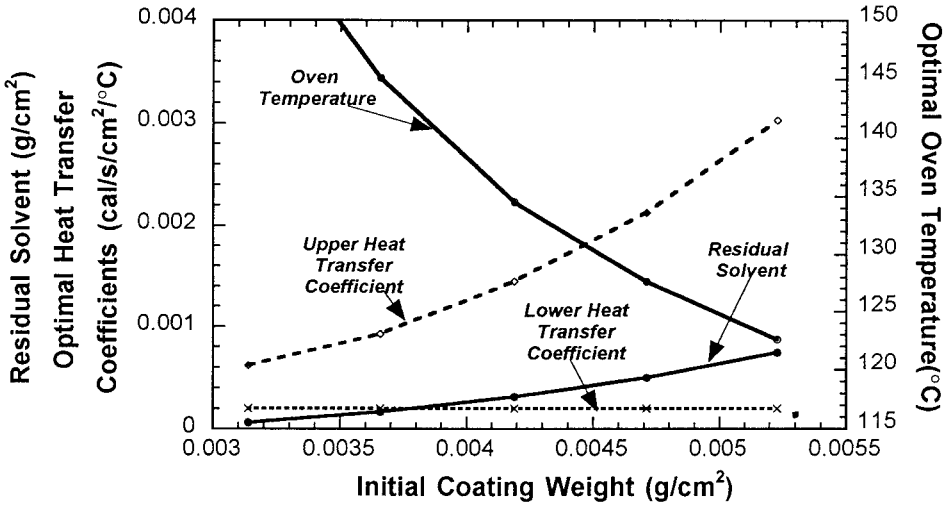

Figure 11 Globally optimal heat-transfer coefficients and oven temperature as a function of coating weight. The coating is initially 40 wt % poly(vinyl acetate) in toluene, and the oven residence time is 30 s.

Table III Optimal Conditions Versus Coating Weight for 40% Solids Solution

Coat Weight (g/cm^2)	h_W (cal s^{-1} cm^{-2} °C^{-1})	h_C (cal s^{-1} cm^{-2} °C^{-1})	T_{oven} (°C)	Residual Solvent (wt %)
3.14×10^{-3}	2×10^{-4}	6.15×10^{-4}	160.0	6.18×10^{-5}
3.66×10^{-3}	2×10^{-4}	9.25×10^{-4}	145.1	1.64×10^{-4}
4.19×10^{-3}	2×10^{-4}	1.44×10^{-3}	134.5	3.07×10^{-4}
4.71×10^{-3}	2×10^{-4}	2.12×10^{-3}	127.6	4.95×10^{-4}
5.23×10^{-3}	2×10^{-4}	3.03×10^{-3}	122.6	7.40×10^{-4}

of *falling-rate* or *diffusion-limited* drying occurs earlier. However, the initial coating is thinner (because the *dry* coating weight is held constant), so the overall effect of increased solids is similar to predrying the coating. Figure 11 and Table III show the dependence of the global optima on the dry coating weight for an initial solids content of 40% by weight (all previous results started at 30% solids). Because there is less solvent in the coatings with higher solids content, there is less total mass, less evaporative cooling, and greater boiling-point elevation. These three effects are similar to the effects of reduction in coating weight and shift the global optima toward lower values of the heat-transfer coefficients and higher temperatures.

Figure 12 and Table IV show how the globally optimal conditions change with the initial solids content for a coating of 4.19×10^{-3} g/cm^2 dry coating weight. Comparison of Figures 12 and 9 show that increasing the solids content has the same effect as does lowering the coating weight. As the percent solids increases, the optimal oven temperature increases gradually, the optimal substrate-side heat-transfer coefficient decreases suddenly to its minimum value, and the optimal coating-side heat-transfer coefficient decreases gradually.

The reasons for these trends in optimum conditions are analogous to the variations with coat weight shown in Figure 9. The lower percent solids solutions have greater total mass, which slows heating, and greater solvent mass, which allows greater evaporative cooling. The lower percent solids solutions also have a higher solvent concentration at the bottom of the coating. Higher solvent concentrations correspond to lower boiling points. These factors combine to shift the optimum conditions for lower solids solutions to higher heat-transfer coefficients but lower oven temperatures.

Solvent Diffusivity

The mutual diffusion coefficient of a solvent in a polymer depends on the physical structure and

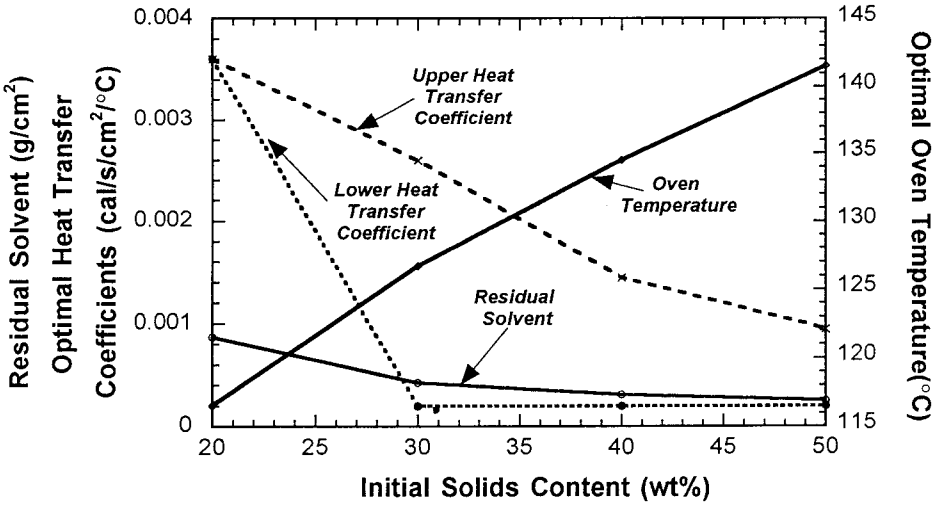

Figure 12 Globally optimal heat-transfer coefficients and oven temperature as a function of initial percent solids in the coating. The poly(vinyl acetate)/toluene coating has a dry coating weight of 4.19×10^{-3} g/cm^2, and the oven residence time is 30 s.

Table IV Optimal Conditions Versus Solids Content for 4.19×10^{-3} g/cm^2 Coating

Solids Content (%)	h_W (cal s^{-1} cm^{-2} °C^{-1})	h_C (cal s^{-1} cm^{-2} °C^{-1})	T_{oven} (°C)	Residual Solvent (wt %)
20	3.6×10^{-3}	3.6×10^{-3}	116.52	8.66×10^{-4}
30	2×10^{-4}	2.59×10^{-3}	126.7	4.22×10^{-4}
40	2×10^{-4}	1.44×10^{-3}	134.5	3.07×10^{-4}
50	2×10^{-4}	9.39×10^{-4}	141.5	2.44×10^{-4}

specific chemical interactions between the polymer and the solvent. The same solvent may diffuse significantly faster in one polymer than in another, and different solvents have significantly different diffusion coefficients in the same polymer. The relative diffusion rates of different solvents in a polymer are not necessarily related to the relative volatilities of those solvents.

The value of solvent diffusivity and its dependence upon concentration and temperature determines the onset of the falling-rate period. Figure 13 and Table V show how the optimal drying conditions from Figure 9 change if the diffusion coefficients are reduced by a factor of 2 ($D_0 = 1.999 \times 10^{-4}$ cm^2/s). The lower diffusivity results in slower drying and higher solvent concentration at the base of the coating. This slows the increase in the bubble-point temperature and causes the optimum conditions to shift toward higher heat-transfer coefficients and lower oven temperatures. Higher heat-transfer coefficients create a higher initial drying rate, but lower oven temperatures cause higher final residual solvents (similar to the example of optimal drying in Figs. 6 and 7).

Oven Residence Time

The position within the oven at which the point of near-blistering occurs can be shifted by changing the web speed or oven residence time. For shorter residence times, thermal effects (heating rate, evaporative cooling, etc.) have greater influence on drying behavior; in a long oven, the coating heats up to the oven temperature in a smaller fraction of the oven length. Figure 14 and Table VI show how the optimal drying conditions versus coating weight change when the oven residence time is cut in half, to 15 s.

In Figure 10, the point of near-blistering occurred between 12 and 20 s depending on coating weight, so the shorter residence time should change the optimal conditions, especially in thinner coatings. For all but the thinnest coating, the

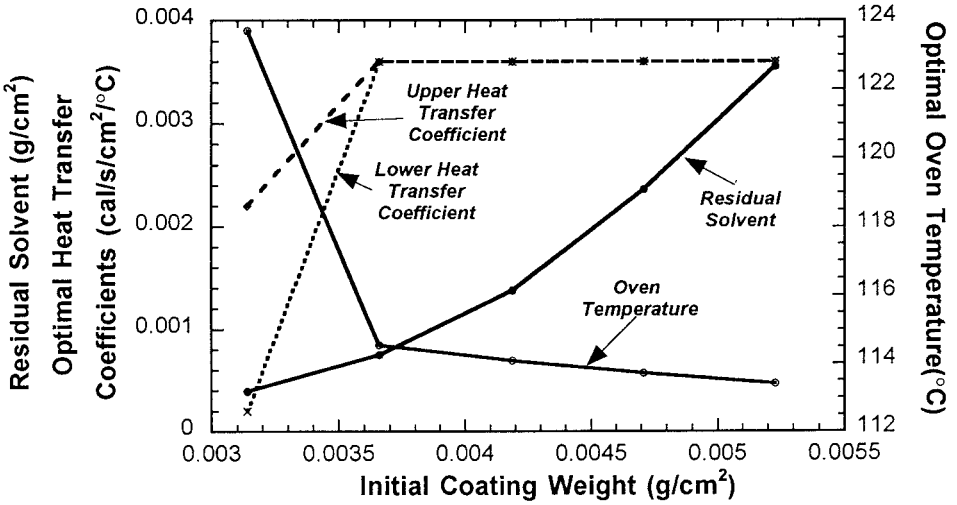

Figure 13 Globally optimal heat-transfer coefficients and oven temperature as a function of coating weight for a solution with a lower diffusivity. The coating is initially 30 wt % poly(vinyl acetate) in toluene, and the oven residence time is 30 s. The parameter D_0 was set to 2×10^{-4} cm^2/s.

Table V Optimal Conditions Versus Coat Weight for Low Diffusivity Coating

Coat Weight (g/cm^2)	h_W (cal s^{-1} cm^{-2} °C^{-1})	h_C (cal s^{-1} cm^{-2} °C^{-1})	T_{oven} (°C)	Residual Solvent (wt %)
3.14×10^{-3}	2.0×10^{-4}	2.2×10^{-3}	123.7	3.91×10^{-4}
3.66×10^{-3}	3.6×10^{-3}	3.6×10^{-3}	114.5	7.50×10^{-4}
4.19×10^{-3}	3.6×10^{-3}	3.6×10^{-3}	114.1	1.38×10^{-3}
4.71×10^{-3}	3.6×10^{-3}	3.6×10^{-3}	113.7	2.36×10^{-3}
5.23×10^{-3}	3.6×10^{-3}	3.6×10^{-3}	113.4	3.55×10^{-3}

globally optimum conditions under a reduced residence time correspond to the maximum coating-side and substrate-side heat-transfer coefficients and oven temperatures slightly above the bubble-point temperature of the initial solution. For the thinnest coating, the globally optimum substrate-side heat-transfer coefficient decreases suddenly and the optimum oven temperature increases suddenly.

For this short residence time, the solvent concentration at the base of the coating does not change significantly except for the thinnest coatings. Thus, there is little elevation in the bubble-point temperature. These conditions favor higher heat-transfer coefficients and lower oven temperatures. Figure 15 shows how the residual solvent, web temperature, and bubble-point temperature vary through the oven for the optimal conditions at 15 s residence times (to compare with Fig. 10 for a 30-s residence time). The profiles for all but the thickest coating change to bring the point of near-blistering earlier within the oven. Thus, shorter ovens will favor higher air flows and lower temperatures.

CONCLUSIONS

This article discussed the application of a detailed mathematical model of heat and mass transfer to drying of polymeric coatings. Similar models have been previously reported by several authors and have been shown to be in good agreement with empirical results. Thus, these models should be effective tools for guiding the design of drying systems and the choice of operating conditions.

We identified two goals in the drying of polymer coatings: (1) minimizing the residual solvent and (2) avoiding blister defects. The operating conditions of the oven temperature, coating-side heat-transfer coefficient, and substrate-side heat-transfer coefficient can be adjusted within practical ranges to find optimal conditions for achieving

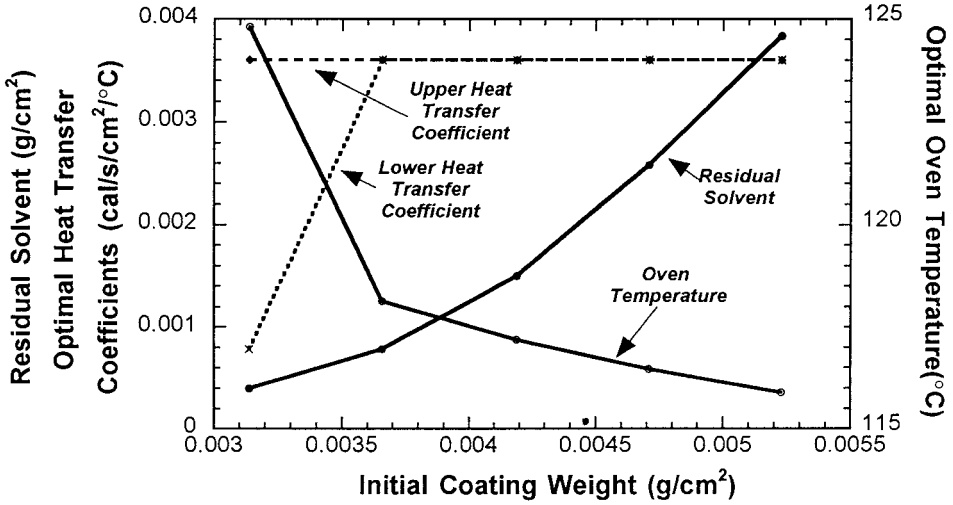

Figure 14 Globally optimal heat-transfer coefficients and oven temperature as a function of coating weight for a shorter oven. The coating is initially 30 wt % poly(vinyl acetate) in toluene, and the oven residence time is 15 s.

Table VI Optimal Conditions Versus Coat Weight for 15 s Oven Residence Time

Coat Weight (g/cm^2)	h_W (cal s^{-1} cm^{-2} °C^{-1})	h_C (cal s^{-1} cm^{-2} °C^{-1})	T_{oven} (°C)	Residual Solvent (wt %)
3.14×10^{-3}	7.82×10^{-4}	3.6×10^{-3}	124.8	3.92×10^{-4}
3.66×10^{-3}	3.6×10^{-3}	3.6×10^{-3}	118.13	7.84×10^{-4}
4.19×10^{-3}	3.6×10^{-3}	3.6×10^{-3}	117.18	1.50×10^{-3}
4.71×10^{-3}	3.6×10^{-3}	3.6×10^{-3}	116.46	2.58×10^{-3}
5.23×10^{-3}	3.6×10^{-3}	3.6×10^{-3}	115.88	3.83×10^{-3}

these two goals. We implemented an automated optimization routine to find the heat-transfer coefficients which produced the lowest residual solvent in a blister-free coating. For our base-case coating, the optimal oven temperature was well above the boiling point of the initial coating solution. The optimum substrate-side heat-transfer coefficient was at the minimum allowable value, corresponding to very gentle parallel air flow. The optimum coating-side heat-transfer coefficient was in the middle of the range of allowable values, corresponding to moderate air impingement.

For all the cases considered, the optimum coating-side heat-transfer coefficient is always equal to or greater than the optimum substrate-side heat-transfer coefficient. This conclusion directly contradicts the common conception that "backside" drying, that is, higher air flow to the backside of the web and lower air flow above the coating, is optimal for maximizing line speed without forming blisters. For some coatings, there may be "near-optimal" conditions with higher substrate-side heat-transfer coefficients, but this is not a general phenomenon.

We also examined how the optimal conditions change with various parameters such as coating weight. In general, any parameter change that causes a delayed decrease in solvent concentration near the base of the film (corresponding to a delayed rise in bubble-point temperature) favors higher heat-transfer coefficients and lower oven temperatures. In other words, any conditions which increase susceptibility to blister formation or increase diffusional resistance to drying favor higher air flows and lower temperatures. Some process changes that are more likely to lead to blistering are thicker coatings, lower percent solids coatings, lower solvent diffusivity, and shorter oven residence times.

The authors would like to acknowledge Sharon Wang and Ilyess Hadj Romdhane from 3M and L. E. Scriven

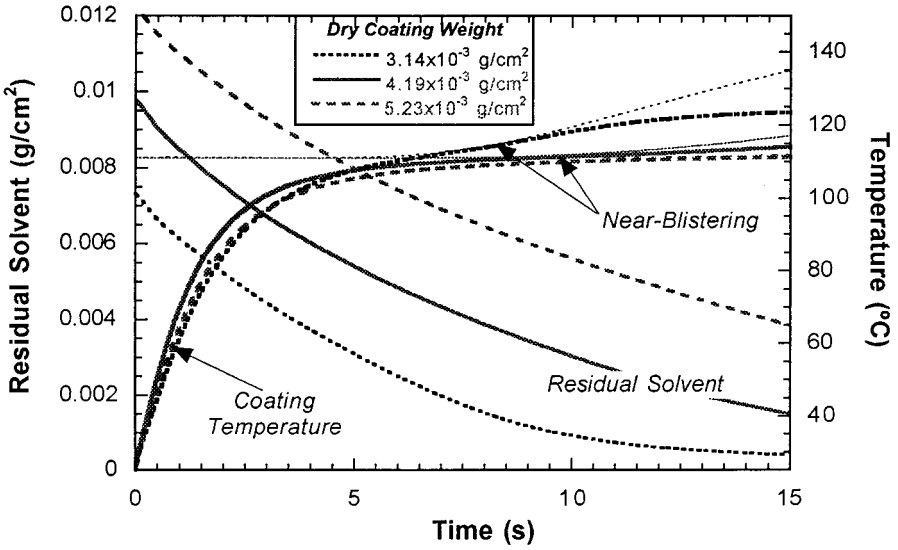

Figure 15 Drying profiles under globally optimal drying conditions for several coating weights corresponding to Figure 14. The oven residence time is 15 s. Bold lines indicate coating temperature and residual solvent, and thin lines indicate bubble-point temperature.

and L. F. Francis at the University of Minnesota for their advice and contribution to this work.

REFERENCES

1. Cohen, E.; Gutoff, E. B. Modern Coating and Drying Technology; VCH: New York, 1992.
2. Robinson, D. E.; Higinbotham, A. E.; Wankat, P. C. Ind Eng Chem Process Des Dev 1969, 8, 502.
3. Roehner, R. Master's Thesis, Ohio University, 1982.
4. Yapel, R. A. Master's Thesis, University of Minnesota, 1988.
5. Cairncross, R. A.; Francis, L. F.; Scriven, L. E. Drying Technol 1992, 10, 893–923.
6. Vrentas, J. S.; Vrentas, C. M. J Polym Sci Part B Polym Phys 1994, 32, 187.
7. Aust, R.; Durst, F.; Raszillier, H. Chem Eng Process 1997, 36, 469–487.
8. Vrentas, J. S.; Duda, J. L. J Polym Sci Part B Polym Phys 1977, 15, 403.
9. Vrentas, J. S.; Duda, J. L. J Polym Sci Part B Polym Phys 1977, 15, 417.
10. Cairncross, R. A.; Jeyadev, S.; Dunham, R. F.; Evans, K.; Francis, L. F.; Scriven, L. E. J Appl Polym Sci 1995, 58, 1279–1290.
11. Dhatt, G.; Touzot, G. The Finite Element Method Displayed; Wiley: New York, 1984.
12. Petzold, L. R. Sandia Laboratories Report, SAND82–8637, 1982.
13. Price, P. E.; Wang, S.; Hadj Romdhane, I. AIChE J 1997, 43, 1925–1934.
14. Garbow, B. S.; Hillstrom, K. E.; More, H. H. LMDIF1, Argonne National Laboratory: Argonne, IL, 1980.